Journal of Computer-Aided Molecular Design, **16:** 601–610, 2002.
KLUWER/ESCOM

Molecular dynamics simulation of cyclosophoroheptadecaose (Cys-A)

Hyunmyung Kim[1], Karpjoo Jeong[2], Sangsan Lee[3] & Seunho Jung[1,*]
[1]*Department of Microbial Engineering,* [2]*College of Information and Communication and* [1,2]*Bio/Molecular Informatics Center, Konkuk University, 1 Hwayang-dong , Gwangjin-gu, Seoul 143-701, South Korea;* [3]*Supercomputing Center in Korea Institute of Science and Technology Information, Yusong-Gu, Eoeun-Dong 52, Daejon 305-806, South Korea*

Received 26 November 2001; accepted in final form 11 October 2002

Key words: conformation; cyclic (1→2)-β-D-glucan; cyclodextrin; cyclosophoroheptadecaose (Cys-A); molecular dynamics simulations; simulated annealing

Summary

The conformational preferences of cyclosophoroheptadecaose (Cys-A), which is a member of a class of cyclic (1→2)-β-D-glucan, were characterized by molecular dynamics simulations. Simulated annealing and constant temperature molecular dynamics simulations were performed on the Cys-A. The simulations produced various types of compact and asymmetrical conformations of Cys-A. Excellent agreement was found between experimental data and corresponding values predicted by molecular modeling. Most glycosidic linkages were concentrated in the lowest energy region of ϕ-ψ energy map, and the values of radius of gyration (R_G) and the nuclear Overhauser effect (NOE) distance data derived from our simulations were finely consistent with the reported experimental values. This result will also give novel insights for the molecular complexation mechanism of Cys-A with various guest chemicals.

Introduction

Cyclic (1→2)-β-D-glucans (known as 'cyclosophoraoses') are a class of unbranched cyclic (1 → 2)-β-D-glucans produced by Gram-negative bacteria of the genera *Agrobacterium* and *Rhizobium*. These compounds vary in size from 17 to 40 glucosyl units [1, 2]. Cyclosophoraoses are known to play an important role in the regulation of osmotic pressure [3] and are involved in the initial stage of root-nodule formation of *Rhizobium* during nitrogen fixation [4]. In this process cyclosophoraoses are suspected to be involved in complexation with various plant flavonoids. Since the first discovery of cyclosophoraoses, much attention has been focused on their biological functions [5] and potential ability to form inclusion complexes with other molecules [6, 7]. Although the significance of the cyclic structure of cyclosophoraoses is not clearly understood, cyclosophoraoses present a challenge in understanding the relationship between their conformations and physicochemical properties.

Because complexation properties are direct consequences of the shape of cyclic oligosaccharides, understanding of their conformation and dynamics in solution is important to study biological functions and to develop technological applications. Many experimental and theoretical attempts have been tried for those purposes. Palleschi and Crescenzi [8] have proposed a symmetrical model for cyclosophoraoses based on the idea of triglucosyl repeat units with a large central cavity. Other researchers have reported more compact conformations of cyclosophoraoses with repeating units [9] or without repeating units [10].

In the present study, we performed simulated annealing molecular dynamics (SA-MD) simulations and constant temperature molecular dynamic simulations on a member of the class of cyclosophoraoses composed of 17 β-D-glucosyl units, namely cyclosophoroheptadecaose (Cys-A). We have investigated overall conformational characteristics, the patterns of

*Corresponding author: E-mail: shjung@konkuk.ac.kr

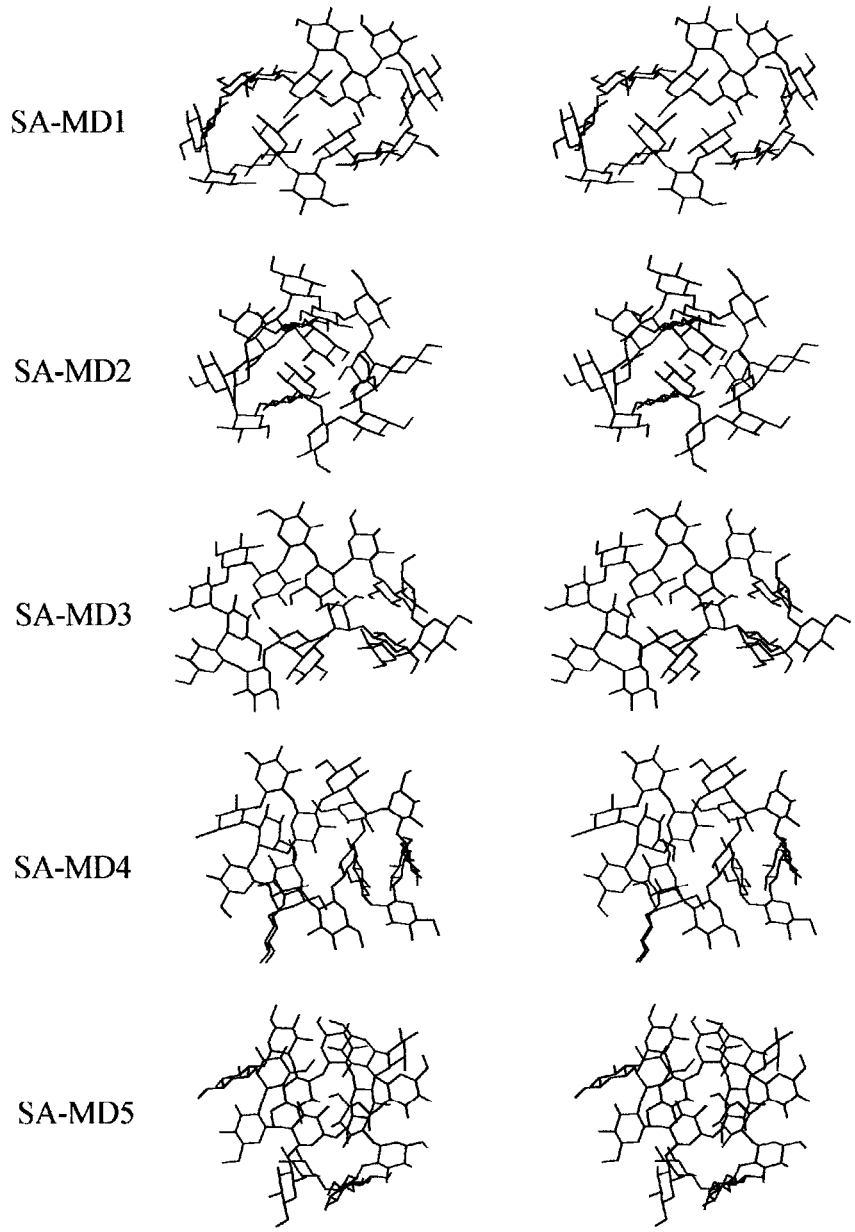

Figure 1. Stereoview of five low-temperature conformers from the SA-MD simulations of cyclosophoroheptadecaose (Cys-A). Each conformation was saved from each production phase at 300 K.

glycosidic dihedral angles, exocyclic torsion of the hydroxymethyl group, the nuclear Overhauser effect (NOE) distance, the radius of gyration (R_G) and the number of intra-molecular hydrogen bonds. Our computer simulations showed excellent agreements to the reported experimental results.

Model and computational procedure

Molecular modeling calculations ware performed with the InsightII/Discover program (version 2000, Molecular Simulations Inc. San Diego, USA). We used the consistent valence force field (CVFF) [11–17]. As the three-dimensional structures of cyclosophoraoses are not available, a molecular model of cyclosophoroheptadecaose (Cys-A) was built using β-D-glucose from

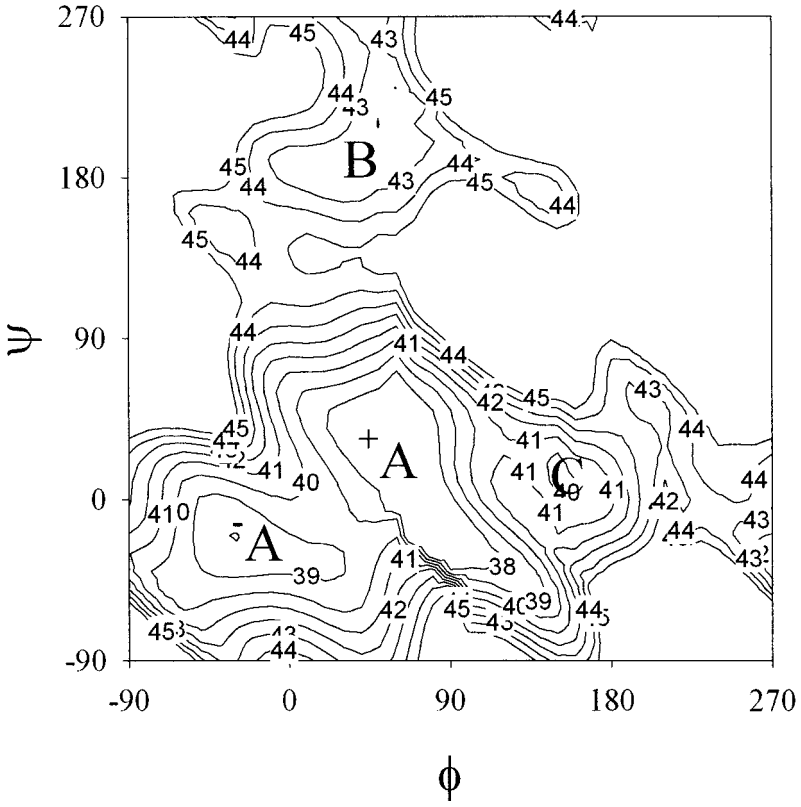

Figure 2. The ϕ-ψ potential-energy map of β-sophorose dimer. The low-energy regions are specified A-, B-, and C- type regions. The contour line corresponds to 1 kcal/mol.

the standard sugar library of the biopolymer module of the Insight II program.

Conformational search of the Cys-A was performed by simulated annealing molecular dynamics (SA-MD) simulations [18]. In SA-MD simulations, the temperature was changed between 300 and 1000 K five times at intervals of 50 K. At each temperature, MD simulations were performed for 7.5 ps: 1.5 ps of equilibration phase and 6 ps of production phase. One structure was saved at the end of each production phase at 300 K. Total MD simulation time was 1057.5 ps. No cut-off was imposed on the calculation of non-bonded interactions. Constant NVT MD calculations were performed using the leap-frog algorithm with a 1 fs time step. The temperature was controlled by velocity scaling in equilibration phases and by the Berendsen algorithm [19] in production phases with a coupling constant of 0.2 ps. The dielectric constant was set to 1. After the SA-MD simulations, the five low-temperature conformations were fully energy-minimized; 100 iterations of steepest descent minimization and conjugate gradient minimization until the maximum derivative reached below 0.05 kcal/mol Å.

To investigate molecular motions of Cys-A at room temperature, molecular dynamics simulations of Cys-A at 300 K were performed in vacuo and in water. In vacuo, the system was equilibrated for 100 ps and production run was carried out for 1000 ps. Intermediate structures were saved every 0.25 ps for analysis. Other MD conditions were same as the SA-MD simulations.

In aqueous environment, Cys-A was solvated with a sphere of 22 Å radius of SPC [20] water molecules (∼1100 water molecules). The solvated Cys-A was energy-minimized and preliminary MD simulations were performed for 50 ps to allow further relaxation of the solvent molecules. Subsequently, the production phase of the MD simulations was done for 1000 ps. The MD calculations were performed using the Velocity Verlet algorithm [21] at constant volume at 300 K. Non-bonded interactions were calculated with fast multipole method [22] implemented in the Discovery program. By constraining bond lengths (rattle algorithm) [23], a time step of 2 fs could be

used. The temperature was controlled using weak coupling to a bath of constant temperature (T = 300 K, τ = 0.1443 ps). Dielectric constant was set to 1. Intermediate structures were saved every 0.25 ps for analysis.

Results and Discussion

Simulated annealing molecular dynamics simulations

Figure 1 shows the five low-temperature conformers of Cys-A obtained from the SA-MD simulations. The overall conformations look quite dissimilar. The root-mean-square displacement (RMSD) between the conformers is in the range of 5–8 Å. These results indicate that a large conformational space was covered during the SA-MD simulations. The ϕ-ψ potential energy map of β-sophorose is shown in Figure 2. The ϕ and ψ glycosidic dihedral angles were defined as ϕ = (H1−C1−O1−C2) and ψ = (C1−O1−C2−H2). The energy contour shows three major low-energy regions; A-, B-, and C-type. A-type region is further divided into two sub-regions; $^{+}$A and $^{-}$A, according to York et al. [9]. A-type region has the lowest potential energy, and B-type region has approximately 6 kcal/mol higher energy than A-type region. The potential energy of C-type region is slightly higher than that of A-type region. Figure 3 shows each low-energy region conformation of β-sophorose. In order to explore the conformational patterns, a Ramachandran-like conformational map of glycosidic dihedral angles, ϕ and ψ, was generated for all the glycosidic dihedral angles of the five conformers of Cys-A [15]. Figure 4 shows that most of the glycosidic dihedral angles adopt the A-type conformation positioned in the lowest-energy region of the potential-energy map.

In Table 1, the overall conformations of each Cys-A obtained from SA-MD simulations were expressed in terms of the type of glycosidic dihedral angles. For each conformer, most of the glycosidic conformations adopted the most stable A-type conformation, and a few dihedral conformations per conformer adopted the less stable B- or C-type conformations.

The radius of gyration (R_G) of Cys-A is a good indicator for the evaluation of simulations. Table 2 shows the R_G of the five conformers of each Cys-A. All the R_Gs are close to the experimentally measured value of 7.8 Å [24].

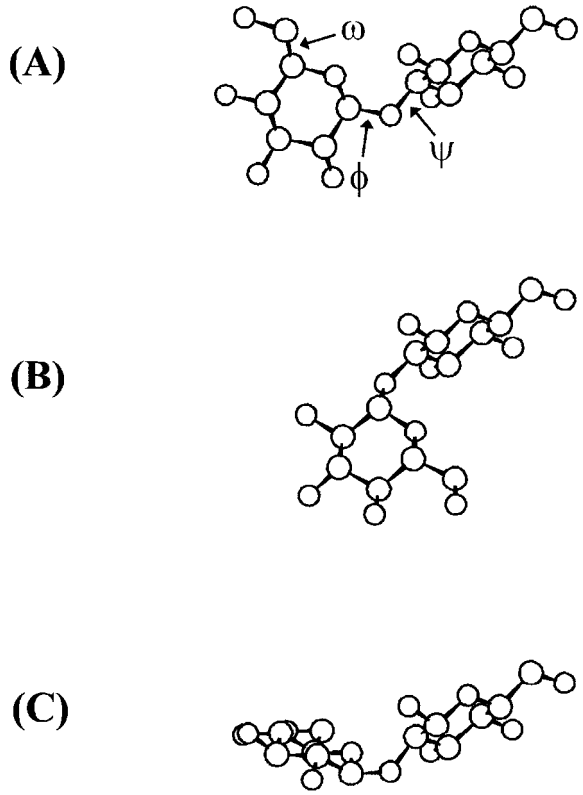

Figure 3. Minimum-energy conformations of β-sophorose dimmer in their low-energy regions. (A) A-type conformation (ϕ = 60°, ψ = 0°), (B) B-type conformation (ϕ = 60°, ψ = 230°), and (C) C-type conformation (ϕ = 150°, ψ = 20°). Each torsional angle was defined as ϕ = (H1-C1-O1-C2), ψ = (C1–O1–C2–H2), and ω = (O5–C5–C6–O6).

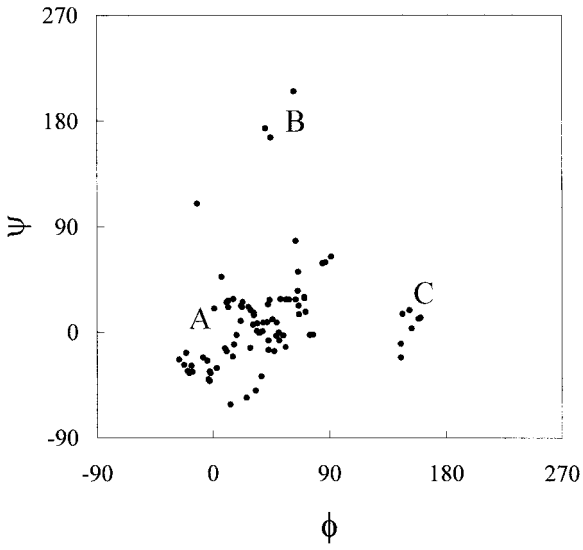

Figure 4. Ramachandran-like conformational map of ϕ-ψ glycosidic dihedral angles, generated for all the glycosidic dihedral angles of the five conformers obtained from SA-MD simulations.

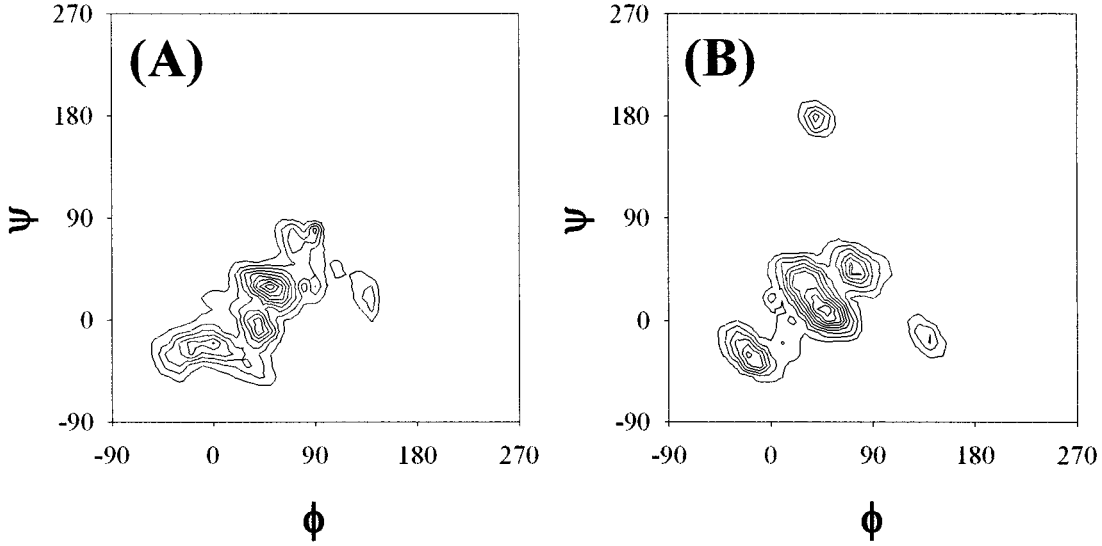

Figure 5. The ϕ-ψ population density map of the glycosidic dihedral angles from the MD simulations in vacuo (A) and in water (B). Contours (lines) correspond to the population densities of 10, 20, 30, 40, 50, 60, 70, 80, and 90% of the maximum value.

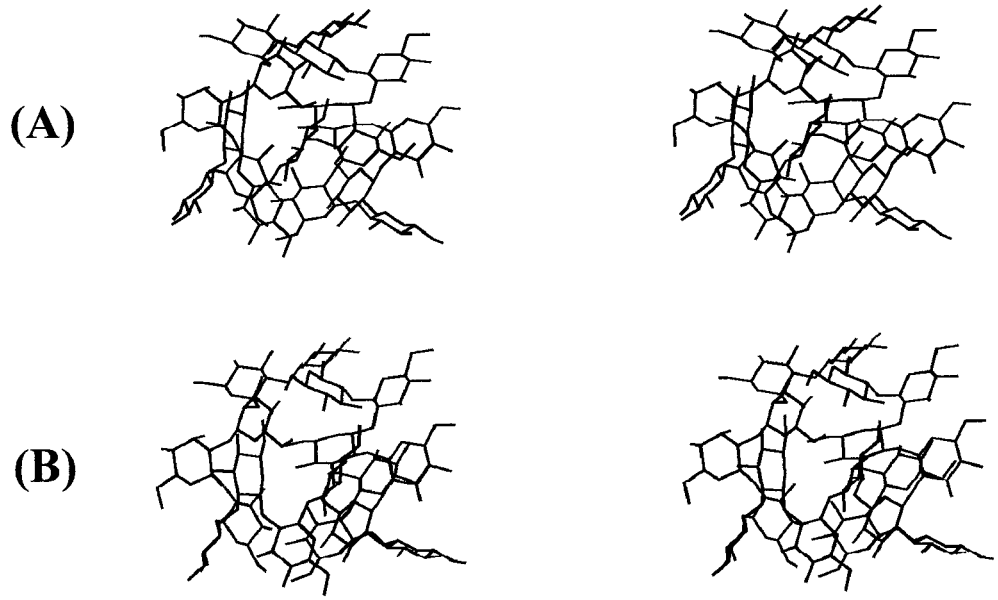

Figure 6. Stereoview of a representative conformation from the MD simulations in vacuo (A) and in water (B).

Molecular dynamics simulations at 300 K in vacuo and in water

We constructed a population density map as a function of dihedral angles (ϕ, ψ) by counting the occurrence in a 10° × 10° angular space for each glycosidic linkage. Figure 5 shows two-dimensional (ϕ, ψ) population density map of the glycosidic dihedral angles. The conformations of glycosidic linkages were concentrated in the low energy regions in both MD simulations. The most prevalent glycosidic linkage was the A-type conformation, and relatively small number of linkages adopted B- and C-type conformations regardless of the condition for MD simulations. Table 1 shows the general conformations of the Cys-A conformers obtained after the MD simulations in terms of three types of glycosidic dihedral angles, A-, B-, and C-type. A representative conformation for each MD simulation is shown in Figure 6.

Table 1. Conformation of each Cys-A conformer from SA-MD simulations, MD simulations in vacuo and in water, expressed in terms of the type of glycosidic dihedral angles.

Conformation	Distribution of A, B and C-type
SA-MD 1	AAAAABAAAAAAAAAAA
SA-MD 2	AAABCAAAAAACACAAA
SA-MD 3	AAACAAAAAAAAAAAAA
SA-MD 4	ACAAAAACAAAAAAAAA
SA-MD 5	AAAABAAAAACAAAAAA
MD in vacuo	AACAAACAAAAAAAAAC
MD in water	AAAABAAAAACAAAAAA

Table 2. Values of R_G after minimization of the conformers of Cys-A.

Conformation	R_G (Å)	Conformation	R_G (Å)
SA-MD1	8.28	MD in vacuo	7.31
SA-MD2	7.32	MD in water	7.90
SA-MD3	8.32	SAXS data[a]	7.80
SA-MD4	7.64		
SA-MD5	7.47		

[a]Ref. 24.

The exo-anomeric effect, which is commonly accepted as being important in determining favored conformations of the glycosidic bond, results in stabilization (for glucopyranosidic bonds with equatorial glycosidic oxygens) of conformations that embody a ϕ angle of 60° or 180° and de-stabilization of conformations having a ϕ angle of $-60°$ [25, 26]. The ϕ angles embodied in the Cys-A structures obtained from the analysis of MD trajectories are considerably in the highly favored 40° to 80° range (Figure 5). The time changes of R_G during the production phase of MD simulations are shown in Figure 7. The stable phases in the last 500 ps were analyzed. The value of R_G in vacuo fluctuated around an average value of 7.3 Å, while the value of R_G in aqueous environment settled into an oscillation around 7.9 Å which is close to the experimental value of 7.8 Å [24]. The presence of water molecules helped to reproduce a more accurate value of R_G compared with simulations in vacuo.

The history of ϕ and ψ for a typical trajectory is given in Figure 8. During the MD simulations, the flexibility of each glycosidic bond was conformationally restricted to a limited area within one of the three low-energy regions. Slight transition of glycoside dihedral angles between A-type and C-type appears in Figure 8 (B), for these two types have similar potential energies as shown in Figure 2. But others do not show any transition at 300 K for this MD simulations. The local fluctuations of ϕ and ψ during the MD simulations were limited to special regions, though irregular shapes were in general observed. The small energy barriers between the low-energy regions were not crossed. This implies that the conformation of β-(1$\rightarrow$2) linkages for Cys-A structures is strongly influenced by the 17-membered ring closure constraints, and thus, each of the Cys-A conformers oscillates in a single potential well. The RMSD between the conformations for the non-hydrogen atoms in this simulations was of order of 2 Å.

The ϕ-ψ potential energy map and population density map of glycosidic dihedral angles showed favored conformational regions similar to those reported by Mimura et al. [24] and York et al. [7] for sophorose from the rigid-residue Monte Carlo sampling analysis. The map is comparable with the relaxed-analysis sophorose model built using an MM3 potential function by Dowd et al. [27]. The lowest-energy A-type conformation is consistent with the conformation of the crystalline form of sophorose hydrate [28]. Throughout the simulations, the glucose units in Cys-A adopted the energetically favorable $^4C_1$ chair conformation [28].

We performed the complete analyses of the exocyclic torsions around C5–C6. Table 3 shows the probability distribution of 17 ω torsional angles (O5–C5–C6–O6) of Cys-A for the last 800 ps trajectories obtained from the MD simulations in water. The exocyclic hydroxymethyl groups in Cys-A existed in three staggered conformations such as *gaushe-gaushe* (GG), *trans-gaushe* (TG), and *gaushe-tran* (GT) [29]. TG conformations were observed as a major rotamer for the seventeen ω torsional angles of hydroxymethyl groups of the Cys-A. The relative probability distribution of each rotamer was changed depending on the position of hydroxymethyl groups inside the Cys-A (Table 3).

The value of R_G from our simulations in water was very close to the reported value of R_G measured by SAXS experiment in aqueous solution [24]. The average value of R_G of MD trajectories in vacuo is smaller than in water (Table 2). Sixteen and eight intramolecular hydrogen bonds were observed in vacuo and in water, respectively (Figure 9). It is likely that the compact conformations with the smaller R_G value

Table 3. Probability distributions of orientations of the hydroxymethyl groups in the MD simulations in water. The torsional angle ω is defined as O5-C5-C6-O6 at each glucose unit in Cys-A, which has seventeen glucose units.

Orientation	ω1	ω2	ω3	ω4	ω5	ω6	ω7	ω8	ω9
TG	86	100	0	29	83	100	63	0	71
GT	14	0	22	71	17	0	37	0	29
GG	0	0	78	0	0	0	0	100	0
Orientation	ω10	ω11	ω12	ω13	ω14	ω15	ω16	ω17	
TG	55	37	10	53	9	3	41	63	
GT	45	63	90	47	34	85	60	37	
GG	0	0	0	0	57	12	0	0	

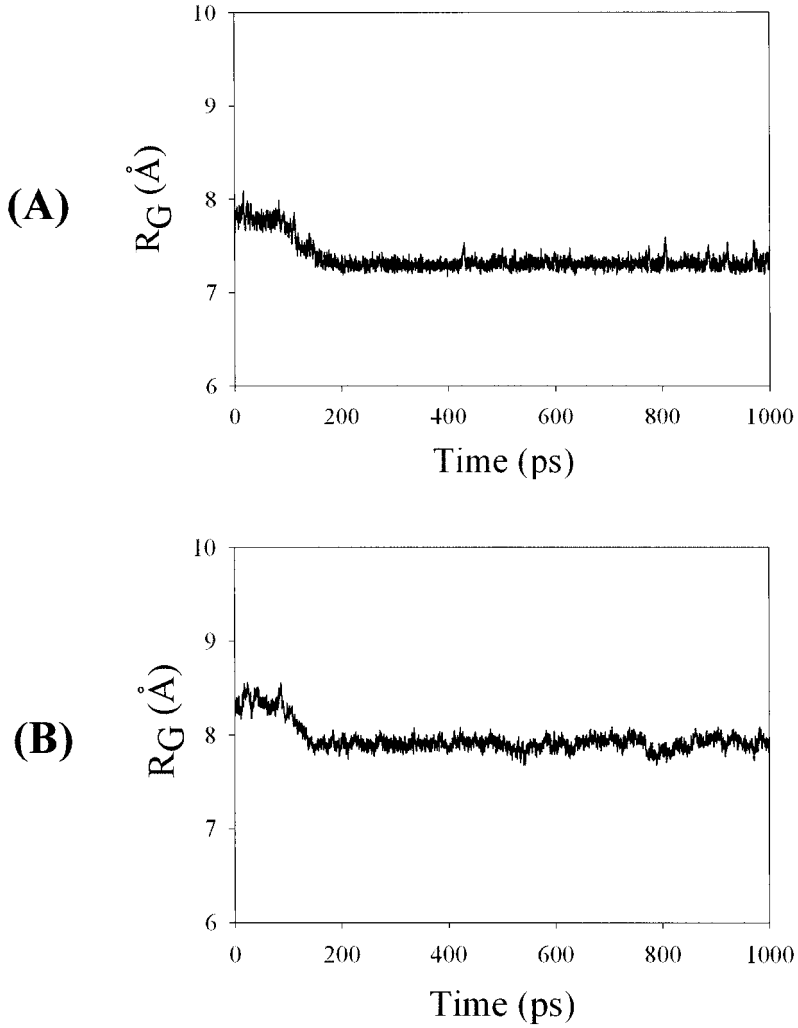

Figure 7. Time changes of R_G during the production phase of the MD simulations in vacuo (A) and in water (B).

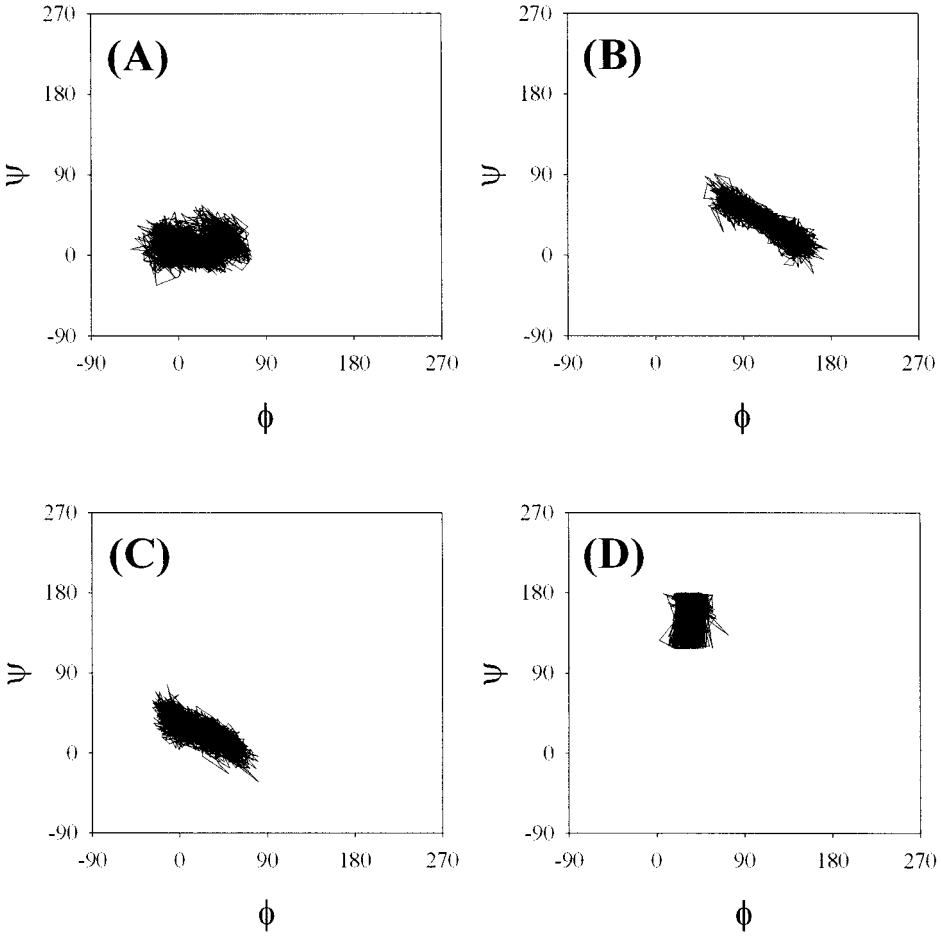

Figure 8. Representative trajectories of Cys-A in the ϕ, ψ space of glycosidic linkage. (A): A-type in vacuo. (B): C-type in vacuo. (C): A-type in water. (D): B-type in water.

have the more intra-molecular hydrogen bonds. In aqueous environment, the number of intra-molecular hydrogen bonds was decreased by formation of the solvent-solute hydrogen bonds. The average R_G value of conformations from the MD simulations in water is closer to that from the SAXS experiment comparing with that from the MD simulations in vacuo.

Table 4 shows the calculated and experimental H1', H2 distances ($R_{H1'-H2}$) estimated from the nuclear Overhauser effect (NOE) distance data [10]. All the calculated values are close to 2.5 Å, which was measured by NMR studies. Especially, the value of $R_{H1'-H2}$ in water is exactly the same as the experimental value, thus finely validating our results.

Based on the simulated conformations of Cys-A, its inclusion complexation seems to act quite differently comparing with typical inclusion complexation, whereas rigid cyclodextrins acted as cyclic host chem-

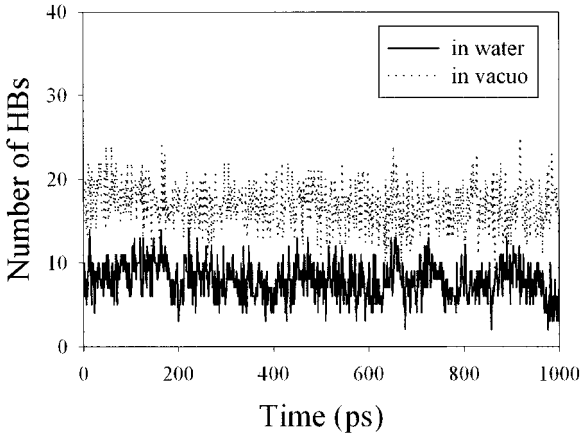

Figure 9. Time changes of numbers of hydrogen bonds (HBs) during the MD simulations. The distance between the donor and the acceptor atom was set within the scope of 2.2 Å [30].

Table 4. Comparison of experimental proton-proton distances $R_{H1'-H2}$ (Å) of Cys-A with the corresponding calculated values.

Conformation	$R_{H1'-H2}$ (Å)
SA-MD 1	2.5
SA-MD 2	2.8
SA-MD 3	2.5
SA-MD 4	2.7
SA-MD 5	2.6
MD in vacuo	2.7
MD in water	2.5
NOE data	2.5[a]

[a]Ref. 10.

icals. The conformations generated from the MD simulations were generally irregular and produced a variety of conformations, indicating the very flexible nature of Cys-A. Particularly, the absence of a distinct hole-like hydrophobic moiety in Cys-A indicates that the molecular mechanism of inclusion complexation by Cys-A must be quite different from that of cyclodextrin (CD) in which there is a clear hydrophobic hole-like conformation. The complexation of guest molecules by Cys-A might be described by a hand-grab type mechanism because a variety of local minima with various conformations may act as fingers in the hand.

Conclusions

In this study, MD simulations were exploited to provide the insight on the conformational features of the Cys-A. This approach produces various types of compact and irregular conformations of Cys-A. Most glycosidic linkages adopted the most stable A-type conformations, as pointed out by other researchers. All the conformations from our simulations had an excellent range of R_G values and $R_{H1'-H2}$ compared with those of experimental data. Our MD simulations might also suggest the possibility of a different molecular mechanism for the complexation by Cys-A from the typical inclusion complexation mechanism by cyclodextrins. Further research is in progress in this view point.

Acknowledgements

This work was supported by grants of Bioproducts and Biotechnology Research Group (01-J-BP-01-B-59) from Ministry of Science and Technology and partially supported by MIC (Ministry of Information and Communication) through National Grid Infrastructure Implementation Project of KISTI (Korea Institute of Science and Technology Information). SDG.

References

1. Abe, M., Amemura, A. and Higashi, S., Plant Soil, 64 (1982) 315.
2. Hisamatsu, M., Amemura, A., Koizumi, K., Utamura, T. and Okada, Y., Carbohydr. Res., 121 (1983) 31.
3. Miller, K.J., Kennedy, E.P. and Reinhold, V.N., Science, 231 (1986) 48.
4. Clarke, H. R., Leigh, J. A. and Douglas, C. J., Cell, 71 (1993) 191.
5. Dylan, T., Nagpal, P., Helinski, D.R. and Ditta, G.S., J. Bacteriol., 172 (1990) 1409.
6. Okada, Y., Horiyama, S. and Koizumi, K., Yakugaku Zasshi, 106 (1986) 240.
7. Kwon, C., Choi, Y., Kim, N., Yoo, J., Yang, C., Kim, H. and Jung, S., J. Incl. Phenom., 36 (2000) 55.
8. Palleschi, A. and Crescenzi, V., Gazz. Chim. Ital., 115 (1985) 243.
9. York, W.S., Thomsen, J.U. and Meyer, B., Carbohydr. Res., 248 (1993) 55.
10. André, I., Mazeau, K., Taravel, F.R. and Tvaroska, I., Int. J. Biol. Macromol., 17 (1995) 189.
11. Hargy, B.J. and Sarko, A., J. Comput. Chem., 14 (1993) 831.
12. Balaji, P.V., Qasba, P.K. and Rao, V.S., Glycobiology, 4 (1994) 497.
13. Asensio, J.L., Martin-Pastor, M. and Jimenez-Barbero, J., Int. J. Biol. Macromol., 17 (1995) 137.
14. Martín-Pastor, M., Espinosa, J.F., Asensio, J.L. and Jimenez-Barbero, Carbohyd. Res., 298 (1997) 15.
15. Chio, Y., Yang, C., Kim, H. and Jung, S., Carbohydr. Res., 326 (2000) 227.
16. Kim, H., Choi, J., Kim, H. and Jung, S., Carbohydr. Res., 337 (2002) 549.
17. Dauber-Osguthorpe, P., Roberts, V.A., Osguthorpe, D.J., Wolff, J., Genest, M. and Hagler, A.T., Proteins, 4 (1988) 31.
18. Choi, Y., Kang, S., Yang, C., Kim, H. and Jung, S., Bull. Korean Chem. Soc., 20 (1999) 753.
19. Berendsen, H.J.C., Postma, J.P.M., van Gunsteren, W.F., DiNola, A. and Haak, J.R., J. Chem. Phys., 81 (1984) 3684.
20. Berendsen, H.J.C., Postma, J.P.M., van Gunsteren, W.F. and Hermans, J., In Pullman B (Ed.) Intermolecular Forces, Reidel, Dordrecht, 1981.
21. Swope, W.C., Anderson, H.C., Berens, P.H. and Wilson, K.R., J. Chem. Phys., 76 (1982) 637.
22. Ding, H.Q., Karasawa, N. and Goddard, W.A., J. Chem. Phys., 97 (1992) 4309.
23. Andersen, H.C., J. Comp. Physics., 52 (1983) 24.
24. Mimura, M., Kitamura, S., Gotoh, S., Takeo, K., Urakawa, H. and Kanjiwara, K., Carbohydr. Res., 289 (1996) 25.
25. Lemieux, R.U., Bock, K., Delbaere, L.T.J., Koto, S. and Rao, V.S., Can. J. Chem., 58 (1980) 631.

26. Bock, K., Pure Appl. Chem., 55 (1983) 605.
27. Dowd, M.K., French, A.D. and Reilly, P.J., Carbohydr. Res., 233 (1992) 15.
28. Ohanessian, P.J., Longchambon, F. and Arene, F., Acta. Crystallogr., Sect B, 34 (1978) 3666.
29. Spieser, S.A.H., van Kuik, J.A., Kroon-Batenburg, L.M.J. and Kroon, J., Carbohydr. Res., 322 (1999) 264.
30. Jeffrey, G.A., An Introduction to Hydrogen Bonding, Oxford, New York, 1997.